Journal of Applied Electrochemistry (2005) 35:347–353
DOI 10.1007/s10800-004-8347-1

Electrochemical impedance study on brass corrosion in NaCl and $(NH_4)_2SO_4$ solutions during cyclic wet–dry conditions

GAMAL A. EL-MAHDY[1,2]
[1]*Department of Metallurgical System Engineering, Yonsei University, 134 Shinchon-dong, Seodaemun-ku, Seoul, Korea, 120-749*
[2]*Chemistry Department, Faculty of Science, Helwan University, Helwan, Cairo, Egypt*
(e-mail: gamalmah2000@yahoo.com)

Received 30 April 2004; accepted in revised form 07 December 2004

Key words: AC impedance, brass, sodium chloride, XRD

Abstract

Atmospheric corrosion of brass in sodium chloride (NaCl) and ammonium sulfate $(NH_4)_2SO_4$ solution during wet/dry cyclic conditions was investigated. The effects of various parameters on the corrosion rate were studied including temperature, pH and surface inclination. The polarization resistance of brass samples, subjected to 1 h immersion and 7 h drying at 60% RH was monitored using an AC impedance. The corrosion rate measured at low temperature was found to be significantly lower than that observed at high temperature. The average reciprocal polarization resistance (V_{ARPR}) was also calculated during exposure. It decreased with the number of exposure cycles during the initial stages and attained a steady state value during the last stage of exposure. An atmospheric corrosion mechanism for brass, describing the successive stages during exposure, is subsequently proposed.

1. Introduction

Copper and its alloys are widely used in many industrial fields, especially in marine applications. Brass alloys are essential materials and meet the industrial requirements as well as commercial applications. A comparative study on the passivation and localized corrosion of α and β – brass immersed in a buffer chloride solution was studied by using X-ray Photo-electron and Auger Electron Spectroscopy [1, 2]. The Passivation of brass was attributed to the formation of a complex passive layer consisting of ZnO and Cu_2O. An increase in chloride concentration produces a substantial decrease in the passive potential and promotes pitting corrosion. The anodic dissolution of β – brass was investigated by using chronoamperometry in Na_2SO_4, NaCl and H_2SO_4 solutions at 30 °C [3]. The corrosion behavior of brass in 0.1 M NaCl solution was investigated using Voltametry [4]. It is assumed that the cuprous chloride complex ion $CuCl_2^-$ accelerates the dezincification of the brass in hydrochloric acid due to catalyzing the dissolution of copper to cupric species [5]. The disproportionation of Cu(1) species into Cu and Cu^{2+} was suggested as a probable process for dezincification in chloride solution [6]. The dezincification of three commercial brasses, with compositions of 70/30, 63/37 and 60/40 (Cu/Zn) in 15.7 N ammonia was evaluated using immersion tests, solution analysis and potentiostatic polarization measurements [7]. The results indicated that the corrosion and dezincification rates increased with corrodent copper concentration. Recently, Multi-analytical *in situ* investigations of the early stages of corrosion of copper, zinc as well as binary copper/zinc alloys were studied in synthetic air with 80% relative humidity (RH) and synthetic air with 80% RH and 250 ppb SO_2 [8]. The experimental results showed that an increase of the zinc content in the brass alloy leads to a dimensional increase of the corrosion features formed on the alloy surface during weathering. AC impedance was applied recently to monitor the atmospheric corrosion of plain carbon steel [9] metals [10–14], weathering steel [15], and coated steel [16, 17].

In previous studies, little attention was paid to the atmospheric corrosion mechanism of brass, studied during wet/dry cyclic conditions. The aim of this work is to gain a better understanding of the corrosion mechanism that brass experiences during wet–dry cycling conditions as well as during variable experimental conditions including: temperature, pH and inclination surface. This work will also investigate the influence of ammonium sulfate solution on the overall corrosion behavior of brass.

2. Experimental

A brass electrode was prepared from 1 mm thick brass sheet with a composition of Cu 70% and Zn 30%. A two electrode-cell, with dimensions of 10 mm × 10 mm was embedded in parallel and 0.1 mm apart, in an epoxy resin and was employed in an impedance measurement. A wet–dry cycle was conducted simulating actual exposure using alternating conditions, which consisted of 1 h immersion in NaCl or ammonium sulfate solutions and 7 h drying time, in a chamber set at 25 °C and 60% RH. The cell was placed horizontally facing upward, in an acrylic vessel. The test solution was introduced into the vessel through an electromagnetic valve, which controlled by using a cyclic on–off timer. The solution was then drained after 1h of immersion using another electromagnetic valve and the specimen was then allowed to dry for 7 h. The electrode was abraded mechanically with SiC paper with differing grades of up to 4000 mesh, and then cleaned with ethanol in an ultrasonic bath.

The polarization resistance measurement was carried out by using an AC impedance Corrosion Monitor (Riken Denshi CT-3) with a multiplexer controlled by a computer through the RS-232 C interface. Impedance was measured at two frequency points of 10 kHz (Z_H) and 10 mHz (Z_L). Polarization resistance Rp was determined by subtracting Z_H from Z_L. A more detailed description of experimental procedure has been presented previously [11, 16, 17].

The composition of the corrosion products was analyzed using X-ray diffraction (XRD), after 72 h of exposure.

3. Results and discussion

3.1. *Influence of pH*

Figure 1 shows the reciprocal of polarization resistance versus the exposure time measured in 0.05 M NaCl solution at pH = 7 and pH = 4 at 60% RH and at 298 K. The reciprocal of polarization resistance is proportional to the corrosion rate [18]. The average of reciprocal of polarization resistance per cycle (V_{ARPR}), which is proportional to the average corrosion rate per cycle, can be calculated by using the following equation:

$$\text{The average of the reciprocal of polarization resistance } (V_{ARPR}) = \int_0^t 1/Rpdt \qquad (1)$$

where t is the time of wetness (TOW). It can be estimated from the data acquired during 1/Rp versus exposure time as the total elapsed time starting from the wetting period to a time just before the completion of surface drying (1/Rp dropped to a value of zero during complete drying of surface). The value of V_{ARPR} was calculated from Equation (1) and is presented in Figure 2 versus the exposure cycle number. The influence of the chloride ion is remarkable in acidic medium (pH = 4) and increases gradually until cycle number 6, and then reaches a steady state value during the last three cycles. The continuous increase in V_{ARPR}

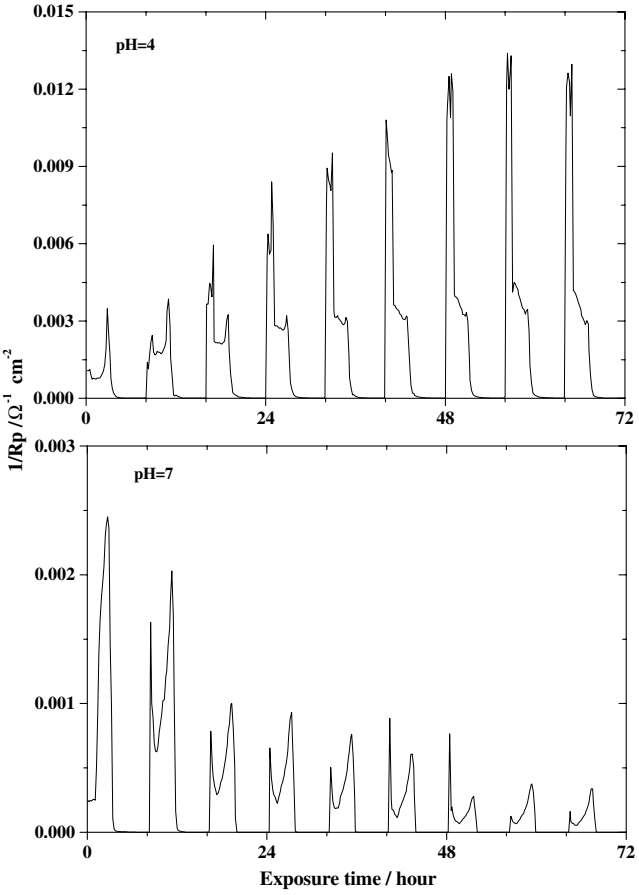

Fig. 1. 1/Rp versus exposure time for brass in 0.05 M NaCl measured at different pH and 60% RH and at 298 K during wet/dry cyclic conditions.

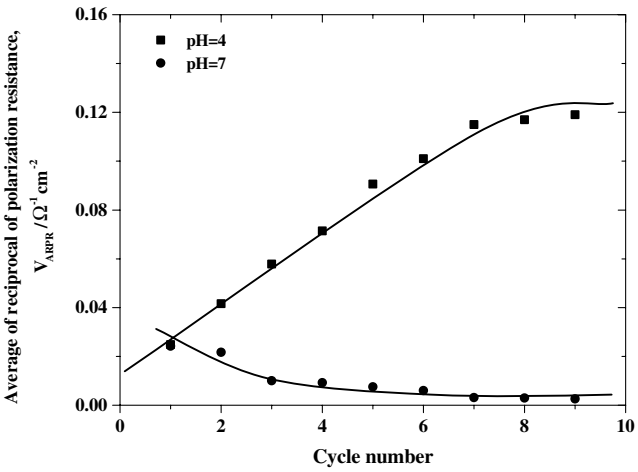

Fig. 2. Dependence of average reciprocal polarization resistance, V_{ARPR}, on pH.

observed with increasing exposure cycle number was attributed to the continuous dissolution of the zinc corrosion product, which subsequently washed away from the surface. The steady state observed during the last stages of exposure was attributed to the formation of stable corrosion products. The compounds identified by X-ray analysis indicate the presence of Cu_2O, Cu, $Cu_2Cl\ (OH)_3$ in the acidic medium. At pH 7, V_{ARPR} decreases rapidly during the first three cycles then more slowly up to the fourth cycle and eventually attains a steady state during the last five cycles. The rapid decrease in V_{ARPR} was attributed to the dissolution of air-formed oxide film. The steady state observed during the last stages of monitoring was attributed to the accumulation of corrosion products, which cover the entire surface. X-ray diffraction indicated the presence of Cu_2O, Cu, $Cu_2Cl\ (OH)_3$, $Zn_5(OH)_8Cl_2\ H_2O$ and ZnO. The higher corrosion rate observed during the initial stage of brass exposure, in the acidic solution than in a neutral solution can be attributed to the higher solubility of ZnO in the acidic medium [19]. Baugh [20] found that the oxide film formed in the pH range 3.8–5.8 was porous and not passivating. A zinc oxide is not stable in the acidic medium and dissolves as [21]:

$$ZnO + 2H^+ = Zn^{2+} + H_2O. \quad (2)$$

The reaction of brass in the acidic solution can be represented by [22, 23]:

$$2Zn_{(Cu-Zn)} + O_2 + 4H^+ = 2Zn^{2+} + 2H_2O \quad (3)$$

$$4Cu_{(Cu-Zn)} + O_2 + 4H^+ = 4Cu^+ + 2H_2O \quad (4)$$

It is assumed that the cuprous chloride ion accelerates the dezincification of brass in the acidic media due to catalyzing the dissolution of copper, which was consequently deposited, at the expense of zinc dissolution [5].

The disproportionation of Cu(I) species into Cu and Cu^{2+} was also suggested as a probable process for dezincification in chloride solution [6, 24, 25].

3.2. *Influence of temperature*

Two experiments were conducted in order to investigate the influence of temperature in 0.025 M NaCl solution at 298 K and 313 K at 60% RH. Figure 3 shows the variation of 1/Rp with exposure time. It is notable that 1/Rp decreases rapidly during the initial stages then more slowly and eventually reaches a steady state value during the last stages of exposure. The V_{ARPR} values were estimated and displayed against the number of exposure cycles as shown in Figure 4. An increase in temperature leads to an increase in the corrosion process. The results may be attributed to the high dissolution process of the brass measured at high temperatures and monitored during the immersion

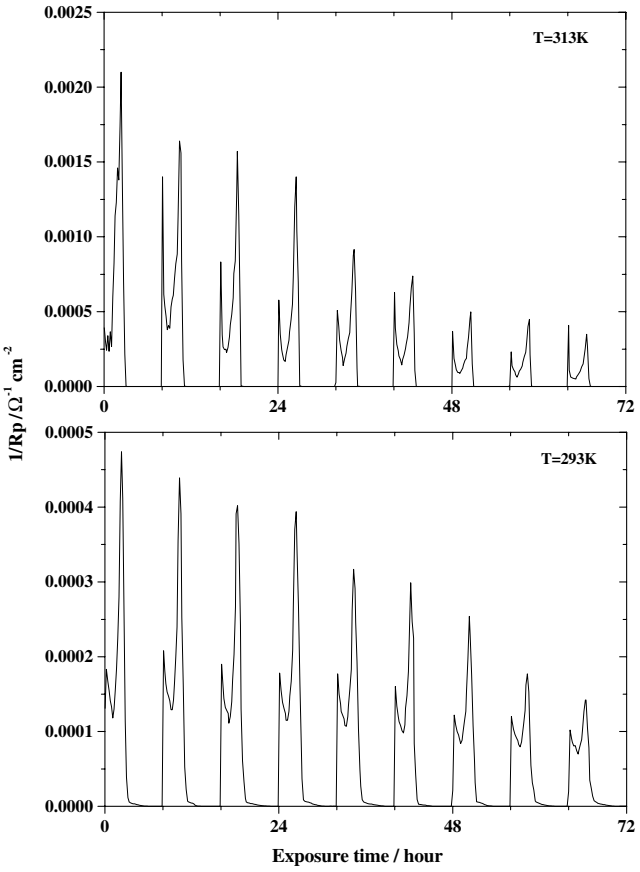

Fig. 3. 1/Rp versus exposure time for brass in 0.025 M NaCl solution measured at different temperatures and 60% RH.

period. These results can also account for the enhancement of the diffusion process of oxygen during the drying period and observed during the thin electrolyte layers. The V_{ARPR} value is high during the first cycle of exposure due to the selective dissolution of zinc during the initial stage of immersion. The lower corrosion rate at low temperature may be attributed to harder, less permeable [26] and adherent [27] corrosion products. In addition, as the temperature increases, the drying time decreases as a result of rapid surface evaporation, which

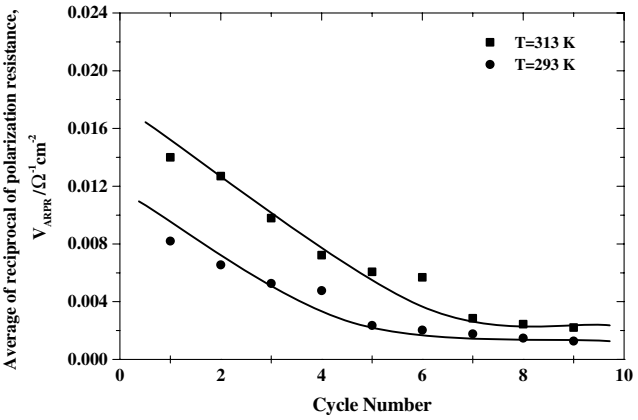

Fig. 4. Effect of temperature on the average reciprocal polarization resistance, V_{ARPR}.

leads to the formation of cracks and defects within the corrosion products. These defectives sites facilitate the diffusion of oxygen through thin electrolyte layers, occurring during the drying period and enhance oxygen reduction. During the last stage of immersion, the amount of corrosion products increased gradually with immersion time. The surface attained a steady state during cycles number 5 and 7 at 293 and 313 K, respectively. This result can be attributed to the low dissolution process of the corrosion products, which leads to the rapid passivation of the surface at 293 K. X-ray diffraction analysis indicated that the films formed on brass were predominantly Cu_2O and $Zn_5(OH)_8Cl_2$ H_2O; this is consistent with the results reported previously for brass tested in tarnishing solutions [28–30] as well as in a marine environment [31]. The results reported previously indicated an increase in the corrosion rate with increase in temperature [32].

3.3. *The influence of surface inclination*

Two experiments were performed in order to investigate the influence of surface inclination measured from the horizontal while immersed in a 0.075 M NaCl solution at 60% RH and at 298 K. The first specimen was placed horizontally facing upward and the second was oriented at 30°. Figure 5 shows the variation of 1/Rp against exposure time. The value of V_{ARPR} is plotted against the number of exposure cycles in Figure 6. V_{ARPR} decreases with surface inclination. This difference in behavior was attributed to the differing TOW, which was estimated from the data shown in Figure 5 and found to be 4.3 h/cycle and 1 h/cycle for the horizontal and the inclined specimen, respectively.

The presence of electrolyte over the surface in the horizontal specimen enhanced the corrosion process during the drying process and the corrosion rate increased as the time of drying progressed, until the surface was completely dried. The thinning process, which occurrs due to the evaporation of electrolyte, leads to enhancement of diffusion and oxygen reduction through the thin electrolyte layers. However, the surface which is passivated during the immersion period (1 h per cycle) in the inclined specimen leads to a decrease in the corrosion rate. During further exposure times, the thickness of the corrosion products increases and effectively reduces the corrosion rate. The greatest determining effect observed for samples exposed at different inclinations is attributed to the difference in TOW.

3.4. *Atmospheric corrosion in an ammonium sulfate solution*

Ammonium and sulfate ions are the most abundant ions existing in fine dust particles commonly found in urban environments, hence an experiment was conducted in 0.01 M $(NH_4)_2SO_4$ solution at 60% RH and at 298 K. Figure 7 shows the variation of 1/Rp with exposure time. Values of V_{ARPR} are presented versus the cycle

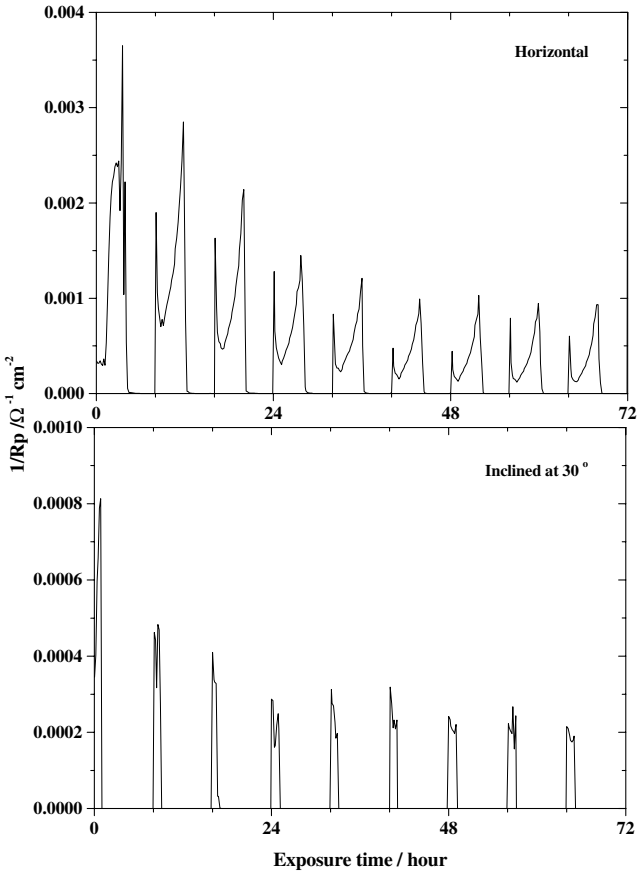

Fig. 5. The variation of 1/Rp with exposure time for a brass surface inclined at 30 ° from the horizon and a horizontally-oriented sample in 0.075 M NaCl at 60% RH and 298 K, during wet/dry cyclic conditions.

number in Figure 8. The corrosion rate is highest during the initial stages due to the dissolution of the air-formed oxide film followed by a dissolution of brass in ammonium solution as [33]:

$$Cu + 2NH_3 \longrightarrow Cu(NH_3)_2^+ + e^- \qquad (5)$$

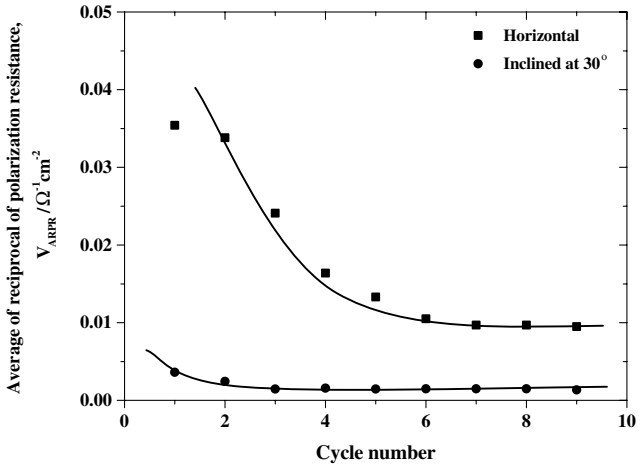

Fig. 6. The influence of surface inclination to 30° from the horizon on the average reciprocal of polarization resistance, V_{ARPR}.

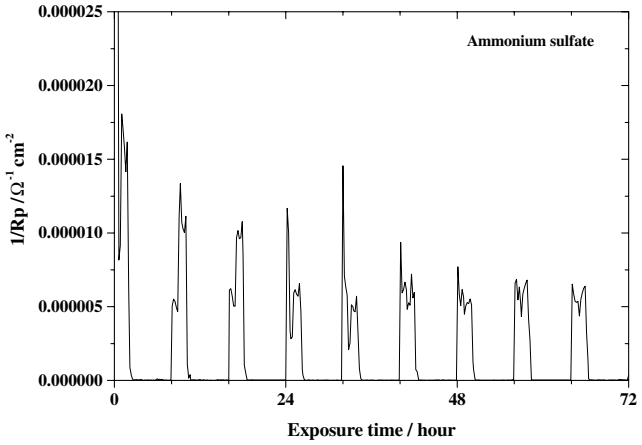

Fig. 7. The variation of 1/Rp with exposure time in 0.01 M $(NH_4)_2SO_4$ solution at 298 K at 60% RH.

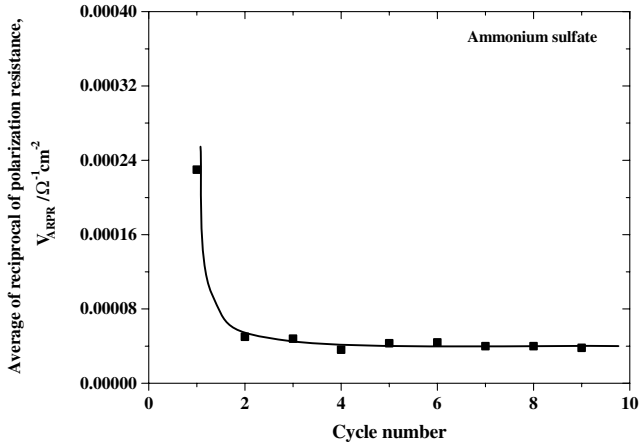

Fig. 8. The variation of average of reciprocal polarization resistance, V_{ARPR}. with cycle number in 0.01 M $(NH_4)_2SO_4$ solution.

$$Zn + 4NH_3 \longrightarrow Cu(NH_3)_4^{2+} + 2e^-$$

The surface attains steady state during cycle four due to the precipitation of hydrated ammonium copper sulfate $(NH_4)_2Cu\ (SO_4)_2 \cdot 6H_2O$, which is identified using X-ray diffraction as a corrosion product.

3.5. *Corrosion behavior within a single wet–dry cycle*

Figure 9 shows the magnified plot of the fifth cycle measured at 313 K in Figure 3. During the first hour immersion in region I, the corrosion rate increases substantially due to the high concentration of NaCl, which precipitated from the fourth cycle. During the drying period in region II the corrosion rate, increases gradually as the drying time progresses. Corrosion rates are greatly accelerated with thin electrolyte layers because of the decrease in diffusion layer thickness, which leads to a higher rate of oxygen reduction. The corrosion rate drops to zero as the surface dries fully during the third period of drying. After completely drying the NaCl chloride and corrosion products started to precipitate over the surface until the onset of the next wetting period (sixth cycle).

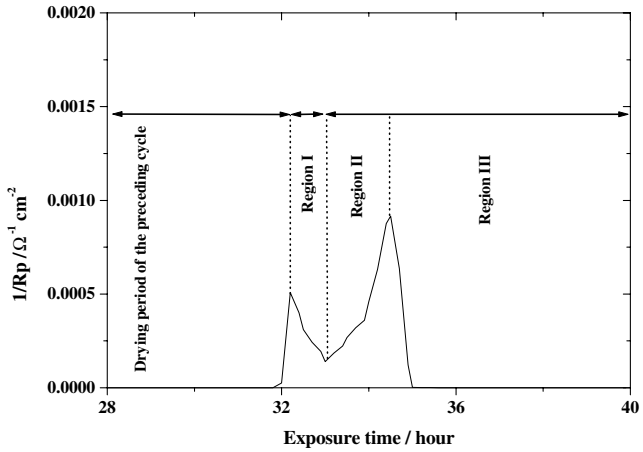

Fig. 9. Monitoring results for a single wet–dry cycle (fifth cycle in Figure 3) showing the variations of 1/Rp versus the exposure time.

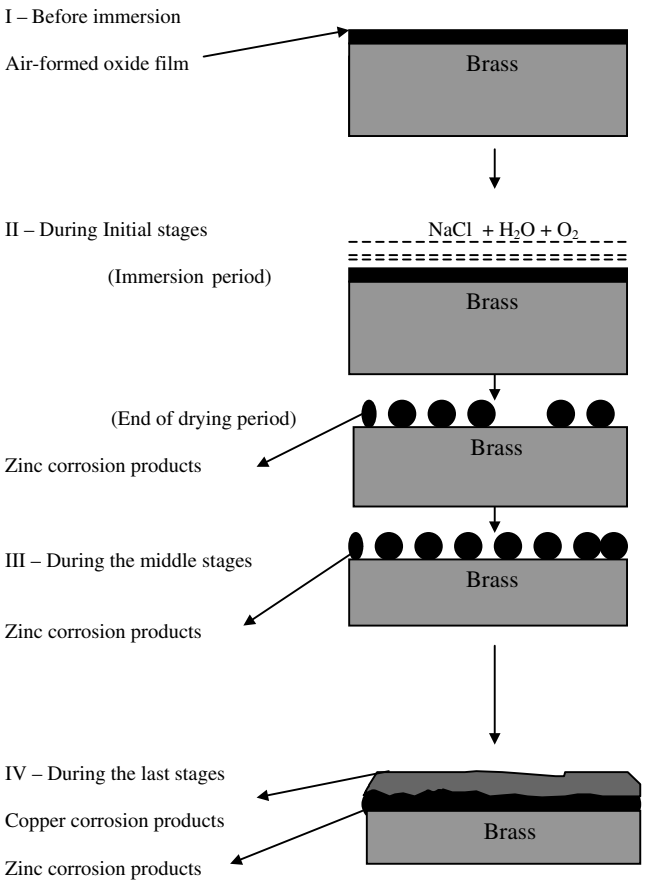

Fig. 10. A Schematic diagram for the mechanism of brass during wet–dry cyclic conditions.

3.6. *Mechanism of Brass corrosion during wet–dry cycling conditions*

The atmospheric corrosion of brass during wet/dry cyclic condition proceeds through the dissolution/re-deposition mechanism. Figure 10 shows the schematic diagram of the corrosion process during wet/dry cyclic conditions. Before immersion (at $t = 0$), the brass surface is covered with a thin layer of air-formed oxide film. The corrosion rate is highest during the initial stages of immersion due to the dissolution of the air-formed oxide film, which is enhanced at high temperature and in acidic medium. Preferential dissolution of zinc occurs as:

$$Zn_{(Cu-Zn)} = Zn^{2+} + 2e^{-} \quad (7)$$

Zinc is released faster than copper due to dezincification leading to surface enrichment of copper. The surface consisted of compounds with different lattice parameters structures, such as Cu_2O $Zn_5(OH)_8Cl_2$, H_2O and ZnO. This heterogeneity reduces the protectivity of the surface film, and promotes de-alloying. During the middle stages of the monitoring process, corrosion products of zinc were formed within the drying period. Parts of these corrosion products were washed away from the surface during the subsequent wetting period while others were retained on the surface. The corrosion of copper started through the porous film of the zinc corrosion products, while the chloride ion penetrated and caused copper corrosion as:

$$Cu_{(Cu-Zn)} = Cu^{2+} + 2e^{-} \quad (8)$$

The cathodic reaction is an oxygen reduction process, which is enhanced during drying with thin electrolyte layers.

$$O_2 + 2H_2O + 4e^{-} = 4OH^{-} \quad (9)$$

During the last stages of exposure the corrosion products of copper formed over the zinc corrosion products and caused a decrease in the corrosion rate. The steady state observed during the last stage of exposure cycles was attributed to complete covering of the surface with corrosion products.

The insoluble corrosion products of zinc are porous and cannot effectively suppress alloy dissolution during the initial stage of monitoring. A protective corrosion product is formed during last stages of monitoring due to the re-deposition of copper corrosion products (Cu_2O, Cu, and Cu_2Cl $(OH)_3$), which cover the entire surface, leading to a decrease in corrosion rate. The outermost part of the corrosion product layer is poor in zinc, due to the initial rapid leaching of zinc [21, 34]. ZnO is also more soluble than Cu_2O in chloride media and hence dezincification is predicted [19]. The lower the corrosion rate, the faster the steady state is achieved as observed at low temperature (from cycles 7 to 9), with an inclined sample (from cycles 4 to 9) and pH 7 (from cycles 6 to 9).

4. Conclusions

1. A ZnO layer provides passivity of brass until is ruptured by dissolution, which leads to a high corrosion rate during the initial stages of immersion.
2. Dezincification is accelerated in an acidic chloride medium, as well as with high temperature.
3. Corrosion of brass monitored during wet/dry cyclic conditions proceeds through a dissolution/re-deposition mechanism.
4. The corrosion rate of brass in ammonium sulfate solution increases during the initial stages then decreases as time progresses, eventually attaining a steady state value during the last stages of monitoring.
5. The inclination of the surface to 30° from the horizontal decreases the total extent of corrosion during a cyclical wet–dry exposure due to electrolyte run-off, which ultimately decreases the TOW.

References

1. J. Morales, G.T. Fernandez, P. Esparza, S. Gonzalez, R.C. Salvarezza and A.J. Arvia, *Corros. Sci.* **37** (1995) 211.
2. J. Morales, G.T. Fernandez, S. Gonzalez, P. Esparza, R.C. Salvarezza and A.J. Arvia, *ibid.* **40** (1998) 177.
3. J.Y. Zou, D.H. Wang and W.C. Qiu, *Electrochim. Acta* **42** (1997) 1733.
4. M. Kabasakaloglu, T. Kiyak, O. Sendil and A. Asan, *Applied Surf. Sci.* **193** (2002) 167.
5. L. Burzynska, A. Maraszewska and Z. Zembura, *Corros. Sci.* **38** (1996) 337.
6. V.F. Lucey, *Br. Corros. J.* **1** (1965) 53.
7. T.K.G. Namboodhiri, R.S. Chaudhary, B. Prakash and M.K. Agrawal, *Corros. Sci.* **22** (1982) 1037.
8. C. Kleber and M. Schreiner, *ibid* **45** (2003) 2851.
9. A. Nishikata, T. Takahashi, H. Bao-rong and T. Tsuru, *Zairyo-to-Kankyo* **43** (1994) 225.
10. A. Nishikata, S. Kumagai and T. Tsuru, *ibid,* **43** (1994) 109.
11. G.A. EL-Mahdy, *Corrosion* **59** (2003) 505.
12. G.A. EL-Mahdy and K.B. Kim, *Electrocim. Acta* **49** (2004) 1937.
13. G.A. EL-Mahdy, K.B. Kim Corrosion, in press.
14. G.A. EL-Mahdy Corros. Sci., in press.
15. A. Nishikata, Y. Yamashita, H. Katayama, T. Tsuru, A. Usami, T. Tanabe and H. Mabuchi, *Corros. Sci.* **37** (1995) 2059.
16. G.A. EL-Mahdy, A. Nishikata and T. Tsuru, *ibid* **42** (2000) 183.
17. G.A. EL-Mahdy, A. Nishikata and T. Tsuru, *ibid* **42** (2000) 1509.
18. M. Stern and A.L. Geary, *J. Electrochem. Soc.* **104** (1957) 56.
19. H.H. Rehan, N.A. Al-Moubarak and H.A. Al-Rafai, *Mater. Corros.* **52** (2001) 677.
20. L.M. Baugh, *Electrochim. Acta* **24** (1979) 657.
21. O. Fruhwirth, G.W. Herzog and J. Poulios, *Surf. Technol.* **24** (1985) 293.
22. T.M.H. Saber and A.A. EL-warraky, *Desalination* **93** (1993) 473.
23. R.K. Dinnappa and S.M. Mayanaa, *J. Appl. Electrochem.* **11** (1981) 111.
24. W.A. Badaway and F.M. Al-Kharafi, *Corrosion* **55** (1999) 268.
25. E. Mattsson, *Electrochim. Acta* **3** (1961) 279.
26. T.P. Hoar and C.J.L. Booker, *Corros. Sci.* **5** (1965) 821.

27. N.D. Tomashov, *Theory of Corrosion and Protection of Metals* (The Macmillan Co., New York, NY, 1966).
28. L.G. Cox, *Ind. Eng. Chem.* **23** (1931) 902.
29. H.E. Johnson and J. Leja, *Corrosion* **22** (1966) 178.
30. C.J.E. Smith and A.N. Hughes, *Br. Corros. J.* **11** (1976) 12.
31. L.M. Gassa and J.R. Vilche, *Corros. Sci.* **25** (1985) 145.
32. P. Stoffyn-Egli, D.E. Buckley and J.A.C. Clyburne, *Applied Chem* **13** (1998) 643.
33. Z. Zembura and M. Opyrchal, *Corros. Sci.* **22** (1982) 1097.
34. U. Bertocci, E.N. Pugh and R.E. Ricker, (edited by R. Gangloff and M. Ives) Environmentally-Induced Cracking of Metals, NACE, 1989, p. 273.